Original Article

MOLECULAR METABOLISM

Brown adipose tissue derived ANGPTL4 controls glucose and lipid metabolism and regulates thermogenesis

Abhishek K. Singh [1,2], Binod Aryal [1,2], Balkrishna Chaube [1,2], Noemi Rotllan [1,2], Luis Varela [2], Tamas L. Horvath [2,3], Yajaira Suárez [1,2,4], Carlos Fernández-Hernando [1,2,4,*]

ABSTRACT

Objectives: Brown adipose tissue (BAT) controls triglyceride-rich lipoprotein (TRL) catabolism. This process is mediated by the lipoprotein lipase (LPL), an enzyme that catalyzed the hydrolysis of triglyceride (TAG) in glycerol and fatty acids (FA), which are burned to generate heat. LPL activity is regulated by angiopoietin-like 4 (ANGPTL4), a secretory protein produced in adipose tissues (AT), liver, kidney, and muscle. While the role of ANGPTL4 in regulating lipoprotein metabolism is well established, the specific contribution of BAT derived ANGPTL4 in controlling lipid and glucose homeostasis is not well understood.

Methods and results: We generated a novel mouse model lacking ANGPTL4 specifically in brown adipose tissue (*BAT-KO*). Here, we report that specific deletion of ANGPTL4 in BAT results in enhanced LPL activity, circulating TAG clearance and thermogenesis. Absence of ANGPTL4 in BAT increased FA oxidation and reduced FA synthesis. Importantly, we observed that absence of ANGPTL4 in BAT leads to a remarkable improvement in glucose tolerance in short-term HFD feeding.

Conclusion: Our findings demonstrate an important role of BAT derived ANGPTL4 in regulating lipoprotein metabolism, whole-body lipid and glucose metabolism, and thermogenesis during acute cold exposure.

Keywords ANGPTL4; Obesity; Lipoprotein metabolism; Glucose tolerance; Thermogenesis

1. INTRODUCTION

Adipose tissue (AT) plays a central role in metabolic homeostasis, obesity, and insulin resistance. The major function of white adipose tissue (WAT) is to regulate lipid storage and mobilization and glucose homeostasis; many functions of WAT in metabolism are exerted by adipose-derived adipokines [1—3]. Dysfunction of adipose tissue is the major contributor to the development of obesity and obesity-associated diabetes [4—6]. In contrast to WAT, brown adipose tissue (BAT) plays an important role in energy metabolism via generating heat by an adaptive process called non-shivering thermogenesis, which requires fuel (fatty acid and glucose) and uncoupling protein 1 (UCP1) [7—9]. Production of heat in BAT is mediated by beta-adrenergic signaling and subsequent uncoupling of ATP production from mitochondrial respiration. BAT allows rodents to maintain body temperature below their thermoneutral zone by dissipating energy as heat [7,10,11]. Under the cold condition, BAT can effectively extract free fatty acids (FFA) derived from circulating triglyceride-rich particles (TRLs) which are its major fuel source [7,12,13]. Therefore, increased BAT activity as a result of cold exposure corrects hyperlipidemia and improves deleterious effects of insulin resistance [12]. However, the mechanisms governing the shuttling of FFAs to BAT is not completely clear. The enzyme lipoprotein lipase (LPL), which is highly expressed in BAT, catalyzes the liberation of fatty acids for fuel in BAT from TRLs [12,14,15]. LPL activity is governed via numerous mechanisms that act primarily at the posttranscriptional and posttranslational level [16,17]. One of the important modulators of LPL activity is angiopoietin-like 4 (ANGPTL4) protein [18—21]. ANGPTL4 is a multifunctional, secreted protein that is highly expressed in WAT, BAT, and macrophages and regulates numerous metabolic processes such as lipid metabolism, glucose homeostasis, and atherosclerosis progression [18,22—24]. Moreover, it has been reported that the expression of ANGPTL4 in mice is regulated by changes in nutritional state in a tissue-specific manner [25]. For example, fasting induces the expression of ANGPTL4 in adipose tissues and liver likely through distinct nuclear receptors PPAR -γ in adipose tissue and glucocorticoid receptor (which is independent of PPAR-α) in liver, whereas feeding exhibits opposite effect [18]. ANGPTL4 protein regulates LPL activity at the posttranscriptional level by interacting directly with LPL and preventing its dimerization and function [20,21]. As a result of its inhibitory action on LPL activity, ANGPTL4 overexpression in mice leads to hypertriglyceridemia, whereas global deficiency leads to increased TAG clearance lowering

[1]Vascular Biology and Therapeutics Program, Yale University School of Medicine, New Haven, CT, USA [2]Integrative Cell Signaling and Neurobiology of Metabolism Program, Department of Comparative Medicine, Yale University School of Medicine, New Haven, CT, USA [3]Department of Anatomy and Histology, University of Veterinary Medicine, Budapest, Hungary [4]Department of Pathology, Yale University School of Medicine, New Haven, CT, USA

*Corresponding author. 10 Amistad Street, Room 337c, New Haven, CT, 06520, USA. Fax: +203 737 2290. E-mail: carlos.fernandez@yale.edu (C. Fernández-Hernando).

Received February 28, 2018 • Revision received March 20, 2018 • Accepted March 23, 2018 • Available online 29 March 2018

https://doi.org/10.1016/j.molmet.2018.03.011

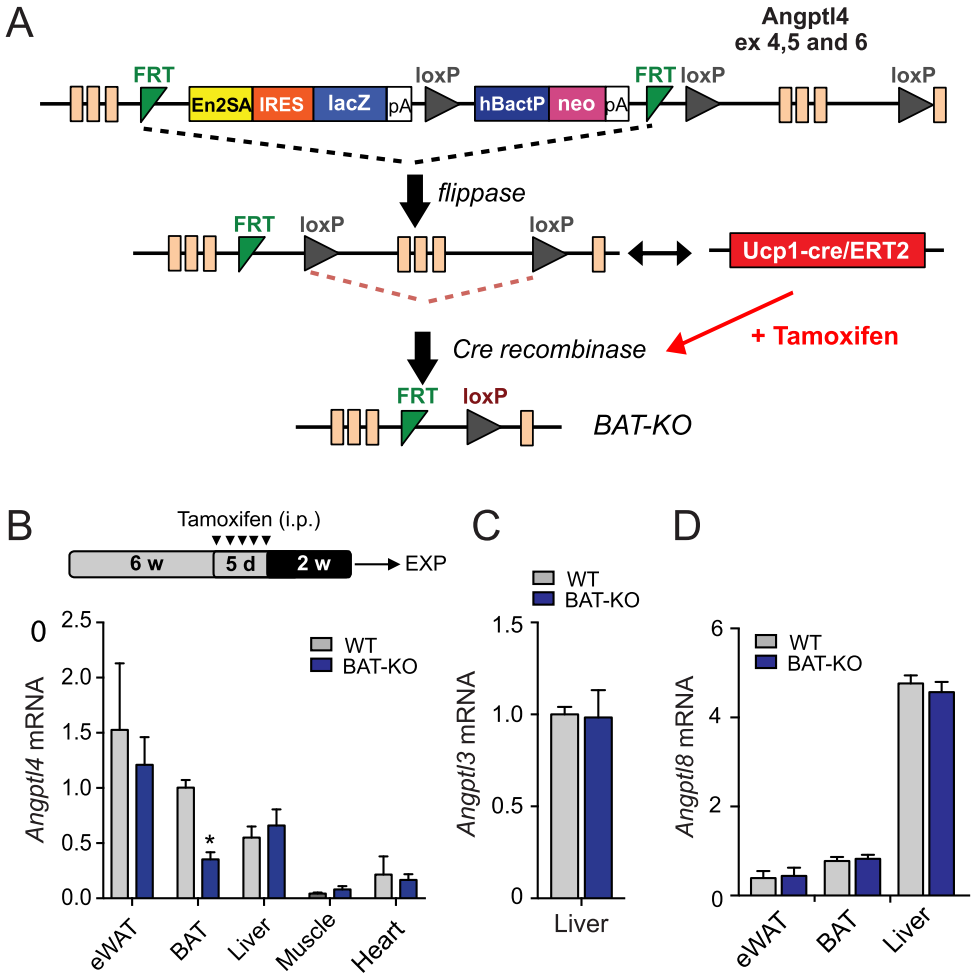

Figure 1: Generation of BAT conditional *Angptl4* knockout mice. (**A** and **B**) Strategy for generating BAT *Angptl4* knockout mice. A "Knock-out first/conditional ready" gene targeting vector was used to generate targeted cells (**A**). To delete the expression of *Angptl4* in BAT *Angptl4*$^{lox/lox}$ mice were bred with Tg (*Ucp1*$^{CRE/ERT2}$) mice and treated with tamoxifen for 5 days (**B**, *upper panel*). (**B**, *bottom panel*) qRT-PCR analysis of *Angptl4* mRNA expression in eWAT, BAT, liver, muscle, and heart isolated from wild-type (WT; *Angptl4*$^{lox/lox}$) and *BAT-KO* (*Angptl4*$^{lox/lox}$ *Ucp1*$^{CRE/ERT2}$) mice (n = 3). *Angptl4* expression in all tissues is normalized to its expression in BAT from WT mice. (**C** and **D**) qRT-PCR analysis of *Angptl3* (**C**) and *Angptl8* (**D**) mRNA expression in eWAT, BAT and liver isolated from wild-type (WT; n = 3) and *BAT-KO* (n = 3) mice. *Angptl8* expression in all tissues is normalized to its expression in BAT from WT mice. Data represent the mean ± S.E.M. and * indicates P < 0.05 comparing BAT-KO with WT mice using unpaired *t*-test.

circulating TAG [26,27]. These observations suggest that BAT specific ANGPTL4 modulation might play an important role in TRL catabolism and BAT activity during cold exposure and development of obesity and insulin resistance (IR). However, the role of ANGPTL4 in obesity and metabolic outcomes is inconclusive as **1**) mice and monkeys deficient in ANGPTL4 exhibit severe metabolic and systemic abnormalities and die prematurely upon high fat diet (HFD) feeding, and **2**) tissue specific targeted modulation of ANGPTL4, which could avoid the complications of global depletion of ANGPTL4 have never been explored due to lack of appropriate animal models.

To investigate the metabolic effect of ANGPTL4 expression in BAT, we generated a novel mouse model lacking ANGPTL4 specifically in BAT (*BAT-KO*). Our results demonstrate that BAT derived ANGPTL4 is an important regulator of lipoprotein metabolism, glucose homeostasis, and insulin sensitivity. Absence of ANGPTL4 in BAT increases TRL catabolism and promotes FA uptake in BAT and cold tolerance upon acute cold exposure. Interestingly, we found that ANGPTL4 deficiency in BAT improves oxidative metabolism, the thermogenic function of brown adipocytes as well as adrenergic independent activation of the peroxisome proliferator-activated receptor γ coactivator 1α (PGC-1α)-uncoupling protein 1 (UCP1) pathway. This noradrenergic activation of PGC-1α and UCP1 pathway may have great significance in anti-obesity and diabetes therapeutics.

2. MATERIALS AND METHODS

2.1. Animals

Male C57BL/6 (*WT*) mice were purchased from The Jackson Laboratory (Bar Harbor, ME, USA) and kept under constant temperature and humidity in a 12 h controlled dark/light cycle. *Angptl4*$^{loxP/loxP}$ mutant mice containing construct with *Angptl4* exons 4, 5, and 6 flanked by loxP sites and lacZ reporter gene and neomycin resistance gene flanked by FRT sites were generated using knock-out first strategy and were purchased from EUCOMM/KOMP repository (Figure 1). ANGPTL4 mutant mice were mated with mice expressing FLP recombinase (JAX stock 009086) to excise the neomycin resistance gene to generate mice with *Angptl4* conditional alleles (*Angptl4*$^{loxP/loxP}$). Homozygous *Angptl4*$^{loxP/loxP}$ mice were crossed with the transgenic mice containing UCP1-ERCre allele obtained from the lab of Dr. Xiaoyong Yang (Yale University) who obtained the original mice from Dr. Christian Wolfrum

(ETH Zurich) to yield offspring inheriting both the targeted allele and the UCP1-ER-*Cre* transgene (*Angptl4*$^{loxP/loxP}$*UCP1*$^{CRE/ERT2}$) generation of UCP1-ERCre mice is described in previous publication [28]. Mice were injected intraperitoneally with tamoxifen (1 mg/mouse/day) at six weeks of age for 5 consecutive days to induce Cre mediated excision of ANGPTL4, specifically in the BAT. Tamoxifen (Sigma—Aldrich) was prepared by solubilizing 20 mg in 1 ml peanut oil (Sigma). Both *Angptl4*$^{lox/lox}$*UCP1*$^{CRE/ERT2}$ (BAT-KO) and *Angptl4*$^{lox/lox}$ littermates obtained equal dose of tamoxifen treatment. Studies were performed 2 weeks after tamoxifen administration. *BAT-KO* mice were verified by PCR with *Cre* primer sequences and primers flanking 5′ homology arm of *Angptl4* gene and LoxP sites using DNA extracted from their tails (Table 1). All experimental mice were housed in a barrier animal facility with constant temperature and humidity in a 12 h dark—light cycle with free access to water and food. All mice were fed a standard chow diet for 8—10 weeks after which were either switched to a high fat diet (60% calories from fat; Research Diets D12492) for 1—20 weeks or maintained on chow diet. All of the experiments were approved by the Institutional Animal Care Use Committee of Yale University School of Medicine.

2.2. Glucose and insulin tolerance test

Glucose and insulin tolerance tests were performed on *BAT-KO* and WT mice that were fasted for 16 h. Glucose concentrations were determined with a Contour Ultra blood glucometer in blood collected from the tail vein at indicated time points. Insulin (0.75 U/kg) for HFD group mice and glucose (1 g/kg) was injected intraperitoneally into mice.

2.3. Fat tolerance test

Fat tolerance test was performed as according to previously described protocol, unless otherwise mentioned [28]. Briefly, mice were fasted for 4 h at room temperature (RT) or at 4 °C were administrated with 10 μl/g body weight of olive oil by oral gavage. TAGs were measured in plasma at the indicated time points.

2.4. Tissue lipid uptake

Measurement of lipid uptake in tissues was performed as previously described [29]. Briefly, mice were fasted for 6 h, at RT or 4 °C and subjected to oral gavage (100 μl) administrated with 100 μl emulsion containing 2 μCi [^{3}H]-triolein. Organs were harvested after 2 h. 50—100 mg pieces of each tissue were weight and lipid were extracted with isopropyl alcohol-hexane (2:3). The lipid layer was collected and [^{3}H]-triolein radioactivity measured by liquid scintillation counting in a beta counter.

Table 1 — Primer sequences.

Genotyping Primers	
ANGPTL4 Flox 1	TGTGGGGTAGGCTTTAGGTG
ANGPTL4 Flox 2	GCTTCTCTCCCTGAGCCTTT
ANGPTL4 Flox 3	GAACTTCGGAATAGGAACTTCG
Cre Primer 1	GCGGTCTGGCAGTAAAAACTATC
Cre Primer 2	GTGAAACAGCATTGCTGTCACTT
Cre Primer 3	CTAGGCCACAGAATTGAAAGATCT
Cre Primer 4	GTAGGTGGAAATTCTAGCATCATCC
qPCR Primers	
ANGPTL4	FW: ACTTCAGATGGAGGCTGGAC
	RE: TCCGAAGCCATCCTTGTAGG
ANGPTL3	FW: GAGGAGCAGCTAACCAACTTAAT
	RE: TCTGCATGTGCTGTTGACTTAAT
ANGPTL8	FW: GCTTTACACCTTCGAGCTGA
	RE: ATCCAGGTAGTCTCAGGCTG
LPL	FW: GGGAGTTTGGCTCCAGAGTTT
	RE: TGTGTCTTCAGGGGTCCTTAG
CD36	FW: TCCTCTGACATTTGCAGGTCTATC
	RE: AAAGGCATTGGCTGGAAGAA
FAS (FASN)	FW: CTTCGCCAACTCTACCATGG
	RE: TTCCACACCCATGAGCGAGT
18S	FW: TTCCGATAACGAACGAGACTCT
	RE: TGGCTGAACGCCACTTGTC

2.5. Hepatic VLDL-TAG secretion

To measure hepatic VLDL-TAG production rate, mice were fasted overnight followed by intraperitoneal injection of poloxamer 407 (1 g/kg body weight) (Sigma—Aldrich) in PBS. Blood was collected via tail bleeding immediately prior to injection and at 1, 2, 3, and 4 h following injection. Triglyceride concentration were measured enzymatically [30].

2.6. Intestinal lipid absorption

To measure intestinal lipid absorption, 6 h-fasted mice were injected with 1 g/kg poloxamer 407. After 1 h, the mice were gavaged with emulsion mixture containing 2 μl [^{3}H]-triolein, and of 100 μl of mouse intralipid 20% emulsion oil. Plasma was collected at the indicated time points. The amount of [^{3}H]-radioactivity was determined in plasma [31].

2.7. LPL activity assay

Post-heparin plasma (PHP) and tissue LPL activity was determined as described previously [28]. In brief, mice were fasted overnight followed by retro-orbital injection of 10 units of heparin/kg body weight. Plasma was separated from blood 5 min after the injection. For measuring total lipase activity, PHP was incubated with 10% Intralipid/[^{3}H]-TAG emulsion as substrate. 1 mM sodium chloride was used in the assay to determine the contribution of hepatic lipase and was subtracted from the total lipase activity to estimate activity of LPL. Heparin-releasable LPL activity in skeletal muscle, heart, and white and brown adipose tissue was measured following the method previously described Haugen et al. Briefly, freshly isolated tissues were weighed and homogenized in ice cold buffer containing PBS with 2 mg/ml of fatty acid free BSA, 5 U/ml heparin, 5 mM EDTA, 1% Triton, 0.1% SDS. Homogenates were centrifuged at 3000 rpm for 15 min at 4 °C and supernatant was used for LPL assay. 100 μl aliquots of the supernatant was used for the lipase activity assay with 100 μl of 10% Intralipid/[^{3}H]-triolein emulsion for 1 h at 25 °C.The activities were normalized for starting tissue weights.

2.8. FA oxidation

Ex vivo FA oxidation in BAT was performed as described previously [32]. Briefly, BAT was isolated from anaesthetized WT and *BAT-KO* mice and homogenized in 5 volumes of chilled STE buffer (pH 7.4, 0.25M sucrose, 10 mM Tris-HCl and 1 mM EDTA). Homogenate was immediately centrifuged, and the pellet was re-suspended followed with incubation with reaction mixture containing medium consist of 0.5 mmol/L palmitate (conjugated to 7% BSA/[^{14}C]-palmitate at 0.4 μCi/ml) for 30 min. Following the incubation, re-suspended pellet containing reaction mixture was transferred to an Eppendrof tube, the cap of which housed a Whatman filter paper disc that had been pre-soaked with 1 mol/L sodium hydroxide. $^{14}CO_2$ trapped in the reaction mixture media was then released by acidification of medium using 1 mol/L perchloric acid and gently agitating the tubes at 37 °C for 1 h. Radioactivity that is being adsorbed onto the filter disc was then quantified by liquid scintillation counting in a beta counter.

2.9. Fatty acid synthase (FASN) activity assay

FASN activity was determined as described previously with slight modifications [33], unless otherwise mentioned. Briefly, BAT from

BAT-KO and WT mice were chopped into fine pieces and homogenized in tissue homogenization buffer (0.1M Tris, 0.1M KCl, 350 mM EDTA and 1M sucrose, pH 7.5) containing protease inhibitor cocktail (Roche, Germany) using tissue homogenizer. Homogenates were clarified by centrifuging at 10,000 rpm for 10 min at 4 °C and kept on ice until the assays are performed. Tissue homogenate was added to assay buffer (100 mM potassium phosphate buffer, pH 7.5 containing 1 mM DTT, 25 μM acetyl CoA, and 150 μM NADPH). FASN reactions were initiated by the addition of 50 μM malonyl-CoA in the reaction buffer. Change in the absorbance at 340 nm was recorded using a spectrophotometer (BioTEK) set in kinetic mode under constant temperature (37 °C).

2.10. Western blot analysis

Tissues were homogenized by physical disruption and the Bullet Blender Homogenizer. Lysis of tissue homogenate was performed in ice-cold buffer containing 50 mM Tris—HCl, pH 7.5, 0.1% SDS, 0.1% deoxycholic acid, 0.1 mM EDTA, 0.1 mM EGTA, 1% NP-40, 5.3 mM NaF, 1.5 mM NaP, 1 mM orthovanadate and 1 mg/ml of protease inhibitor cocktail (Roche), and 0.25 mg/ml AEBSF (Roche). Lysates were sonicated and rotated at 4 °C for 1 h followed by separation of insoluble material by centrifugation at 12,000 × g for 10 min. Lysates were resuspended in SDS sample buffer after normalizing the protein concentration. Samples were separated by SDS—PAGE. Nitrocellulose membranes were used to transfer the proteins and were probed with the indicated antibodies: anti-PGC-1α (Santa Cruz, Sc-13067, 1:1000), anti-UCP1 (abcam, ab10983, 1:1000), and anti-β-actin (GeneTex, GTX629630, 1:5000). Protein bands were visualized using the Odyssey Infrared Imaging System (LI-COR Biotechnology) and densitometry was performed using ImageJ software. For western blot analysis of ApoB-100 and ApoB-48 in pooled lipoprotein fractions, separation was performed on a NuPAGE Novex 4—12% Tris-Acetate Mini Gel using 1x NuPAGE Tris-Acetate SDS running buffer (Invitrogen). The membranes were probed with an antibody against ApoB (Meridian, #K23300R, 1:2000) overnight at 4 °C and visualized as above.

2.11. RNA isolation and quantitative real-time PCR

Total RNA was isolated from tissue using TRIzol reagent (Invitrogen) following manufacturer's protocol. For analyzing mRNA expression, cDNA was synthesized from mRNAs using iScript RT Supermix (Bio-Rad), according to manufacturer's instructions. Quantitative real-time PCR (qRT-PCR) was performed in duplicate using EvaGreen Supermix (BioRad) on an iCycler Real-Time Detection System (Eppendorf). The mRNA levels were normalized to 18S. The sequences of all the primers used for qRT-PCR are provided in Table 1.

2.12. BAT H&E staining

Fresh BAT was fixed with paraformaldehyde and embedded in paraffin. Deparaffinized and hydrated BAT sections (5 μm) of WT and *BAT-KO* mice were stained with hematoxylin-eosin (H-E).

2.13. Lipoprotein profile and lipid measurements

For determining the lipoprotein profile and lipid level, mice were fasted for 12—16 h overnight before collecting blood by tail bleeding, followed by separation of plasma by centrifugation. Plasma was precipitated using HDL-Cholesterol E precipitating reagent (Wako, Japan), and the supernatant was collected as HDL-C fraction. Levels of total cholesterol and TAGs were measured in plasma based on enzymatic reactions following manufacturers' instructions (Wako Pure Chemicals Tokyo, Japan). To determine the lipid distribution in plasma lipoprotein fractions, fast performance liquid chromatography was performed using

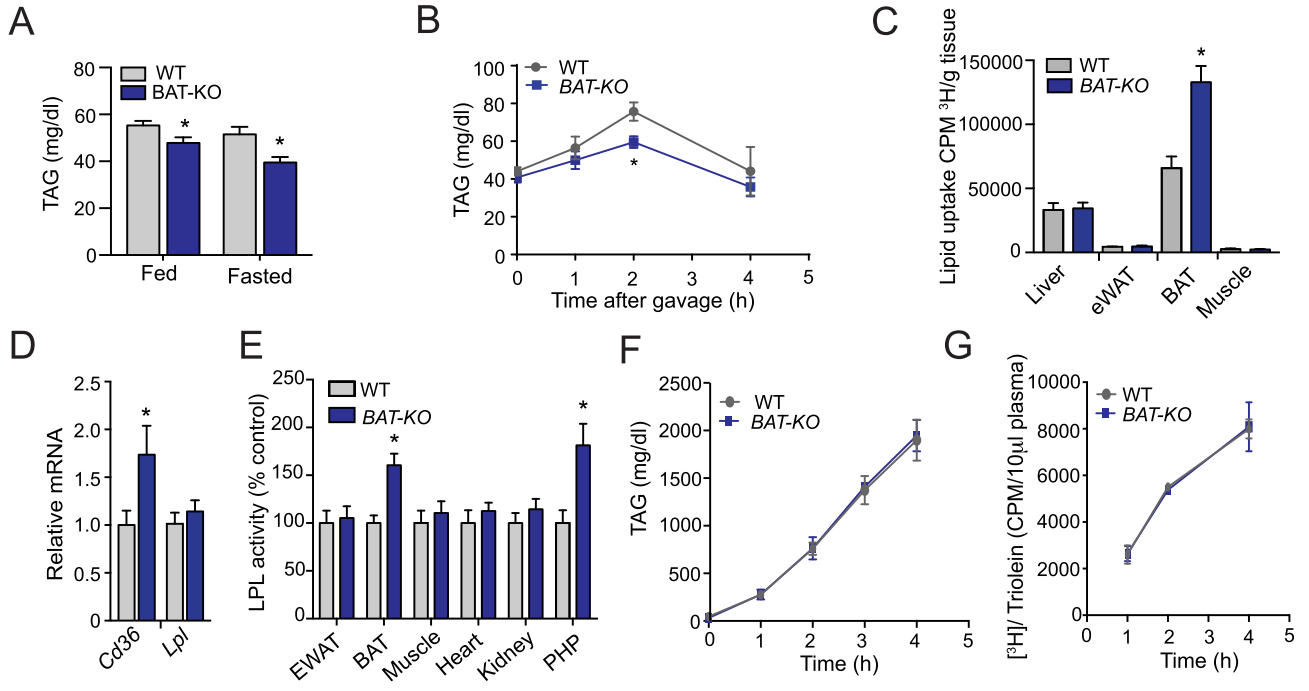

Figure 2: Genetic loss of *Angptl4* in BAT enhances plasma TAG clearance and tissue lipid uptake. (**A**) Fed and fasted plasma triacylglyceride (TAG) levels in WT and *BAT-KO* mice (n = 5). (**B**) Oral lipid tolerance test in 4 h fasted WT and *BAT-KO* mice followed by an oral gavage of olive oil (n = 5). (**C**) Radioactivity incorporation in indicated tissues after 2 h of oral gavage of [^{3}H]-triolein in 6 h fasted WT or *BAT-KO* mice (n = 6). (**D**) qRT-PCR analysis of *Cd36* and *Lpl* mRNA expression in BAT isolated from WT and *BAT-KO* mice (n = 3). (**E**) LPL activity in the indicated tissues isolated from WT and *BAT-KO* mice. Plasma LPL activity was assessed from blood isolated 5 min after heparin injection (n = 3). (**F**) Circulating TAG from WT and BAT-KO mice fasted for 4 h and treated with the LPL inhibitor, poloxamer 407 (n = 3). (**G**) Plasma ^{3}H counts after injection of poloxamer 407 combined with an oral lipid gavage containing [^{3}H-triolein (n = 3).

gel filtration with 2 Superose 6 HR 10/30 columns (Pharmacia Biotech, Uppsala, Sweden).

2.14. Cold tolerance test

For acute cold tolerance test, mice were kept under cold condition with temperature fixed at 4 °C, without food. Rectal temperature was measured using BAT-12 microprobe thermometer (Physitemp) at indicated time points.

2.15. Statistical analysis

Statistical analysis was performed using GraphPad Prism Software Version 7 (GraphPad, San Diego, CA). Data are expressed as mean ± SEM. Statistical differences were measured using an unpaired two-sided Student's *t*-test, or one-way ANOVA with Bonferroni correction for multiple comparisons. The number of animals used in each study is listed in the figure legends. No inclusion or exclusion criteria were used and studies were not blinded to investigators or formally randomized. A value of $p \leq 0.05$ was considered statistically significant.

3. RESULTS

3.1. Generation of brown adipose tissue-specific ANGPTL4 knockout mice

To define the specific contribution of ANGPTL4 in BAT, we generated a mouse model with inducible brown adipocyte-specific deletion of ANGPTL4 (*Angptl4*$^{lox/lox}$*Ucp1*$^{CRE/ERT2}$) indicated as *BAT-KO* (Figure 1A). Treatment of mice with tamoxifen (TMX) induced effective deletion of *Angptl4* in BAT depot of mice carrying *Ucp1*$^{CRE/ERT2}$ (*Angptl4*$^{loxP/loxP}$*Ucp1*$^{CRE/ERT2}$) but not in TMX-treated mice lacking *Ucp1*$^{CRE/ERT2}$ allele. As a consequence of the deletion, *BAT-KO* mice had ~70% reduction of *Angptl4* mRNA levels in BAT (Figure 1B). We also analyzed the expression of *Angptl4* in other tissues such as eWAT, liver, muscle, and heart; however, its expression was found to be unaltered in these tissues of BAT-KO mice as compared to those of WT mice (Figure 1B). Apart from ANGPTL4, other members of angiopoietin like protein (Angptl) family including ANGPTL3 and ANGPTL8 also inhibit LPL activity [34]. To determine whether the loss of ANGPTL4 in the BAT is compensated by other Angptls, we compared the expression of *Angptl3* and *Angptl8* in liver and adipose tissue (WAT and BAT) of WT and BAT-KO mice. The expression of *Angptl3* was undetectable in the adipose tissues while its expression in liver was not different between two groups of mice (Figure 1C). Similarly, expression of *Angptl8* was unaltered in liver, BAT, and WAT of BAT-KO mice as compared to its counterpart (Figure 1D).

3.2. Genetic loss of ANGPTL4 in brown adipocytes exhibited improved plasma TAG tolerance and tissue lipid uptake

To determine the impact of ANGPTL4 depletion in brown adipocytes, we assessed plasma TAGs in 2-month-old *BAT-KO* CD-fed mice. A marked decrease in circulating TAG was observed in the *BAT-KO*

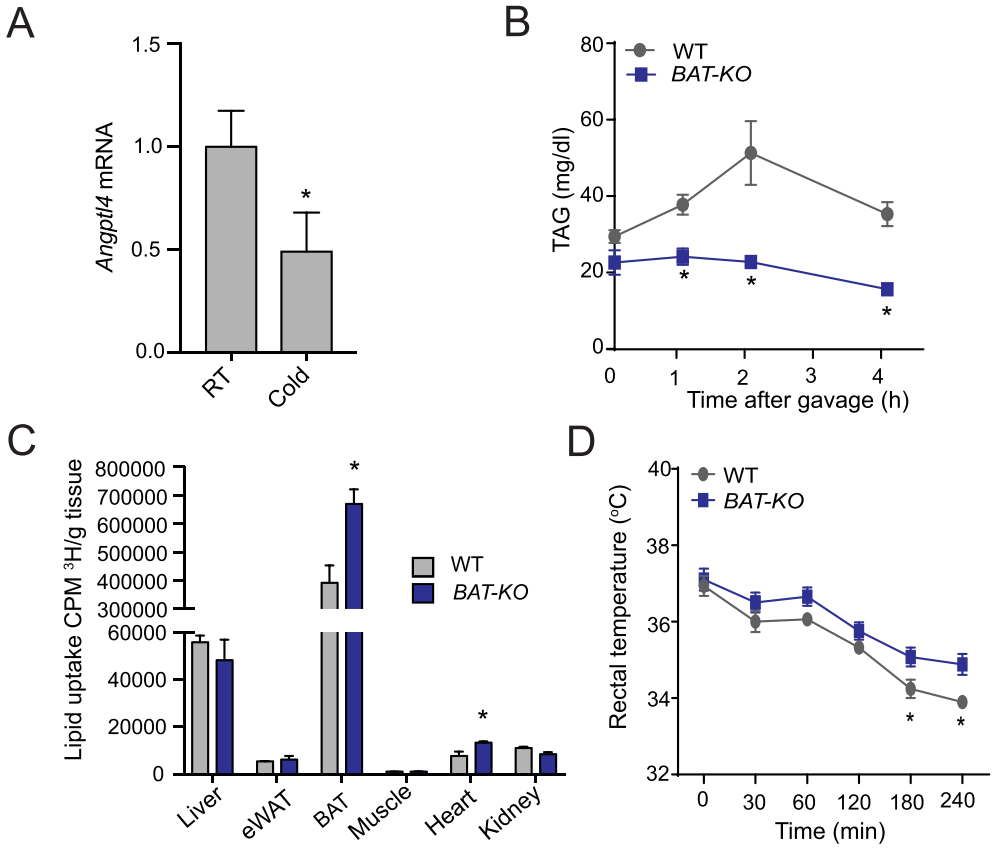

Figure 3: Lack of ANGPTL4 in BAT stimulates FA uptake in BAT and augments thermogenesis upon acute cold exposure. (**A**) *Angptl4* mRNA in BAT lysates of WT mice exposed to 4 °C or RT for 4 h. (**B**) Plasma TAG levels during oral lipid tolerance test in fasted WT and *BAT-KO* mice during acute cold exposed setting (n = 5). (**C**) Tissue distribution of [^{3}H] after 2 h oral gavage of [^{3}H]-triolein (n = 3) in acute exposed condition. (**D**) Body temperature analysis in *BAT-KO* and WT mice in an acute cold exposed setting (n = 5). Mice had no access to food during the experiments performed in panel **A**–**D**. All data represent the mean ± S.E.M. and * indicates P < 0.05 comparing *BAT-KO* with WT mice using unpaired *t*-test.

mice under fed as well as fasted conditions (Figure 2A). Here, we speculated that decreased plasma TAGs could be caused either by decreased entry of TAGs into plasma as hepatic VLDL production or chylomicron (*intestinal absorption*) or increased TRL catabolism. Available evidence suggests that the absence of ANGPTL4 activates LPL, leading to increased plasma TAG-hydrolysis and concomitant TAG clearance from circulation. Therefore, to assess how depletion of ANGPTL4 in BAT influences TAG clearance, we performed fat tolerance test. Expectedly, accelerated plasma TAG clearance was observed in *BAT-KO* mice but not in WT mice after olive oil gavage (Figure 2B). To further explore whether ANGPTL4 could enhance TAG hydrolysis and FA uptake in BAT, we performed lipid uptake experiment with intralipid mixed with [^{3}H]-triolein. Lowering of plasma TAGs level after 2 h oral gavage was associated with a greater uptake of [^{3}H]-triolein in the BAT but not in other organs such as liver, muscle, and WAT (Figure 2C). These observations indicate a possible involvement of FA transporters as well as LPL in the selective enhancement of lipid uptake in BAT. We analyzed the expression of *Cd36* (FA transporter) and *Lpl* in BAT of both groups of mice. Noticeably, we found an increased expression of *Cd36* in the BAT of BAT-KO mice as compared to WT (Figure 2D). However, the mRNA levels of *Lpl* in the BAT were unaltered (Figure 2D). Next, we checked the changes in LPL activity across different tissues as a result of ANGPTL4 deletion in BAT. We found a marked increase in LPL activity in BAT and post-heparin plasma (PHP) in BAT-KO mice as compared to its counterpart (Figure 2E). Moreover, it is known that the level of circulating TAG is dependent on relative rate of VLDL and chylomicron production and LPL-mediated TRL catabolism [14,35]. Thus, to examine whether the expression of ANGPTL4 in BAT influences circulating TAG by altering hepatic VLDL production, we evaluated rates of liver VLDL-TAG production in *BAT-KO* mice. No significant difference was observed in the rate of hepatic VLDL production in WT and *BAT-KO* mice (Figure 2F). Similarly, intestinal lipid absorption was comparable in WT and *BAT-KO* (Figure 2G), suggesting that the reduced circulating level of TAG in *BAT-KO* mice is likely mediated by enhanced TRL catabolism in BAT. Together, these results indicate that BAT-derived ANGPTL4 controls lipoprotein metabolism, circulating TAG clearance, and FA uptake in BAT.

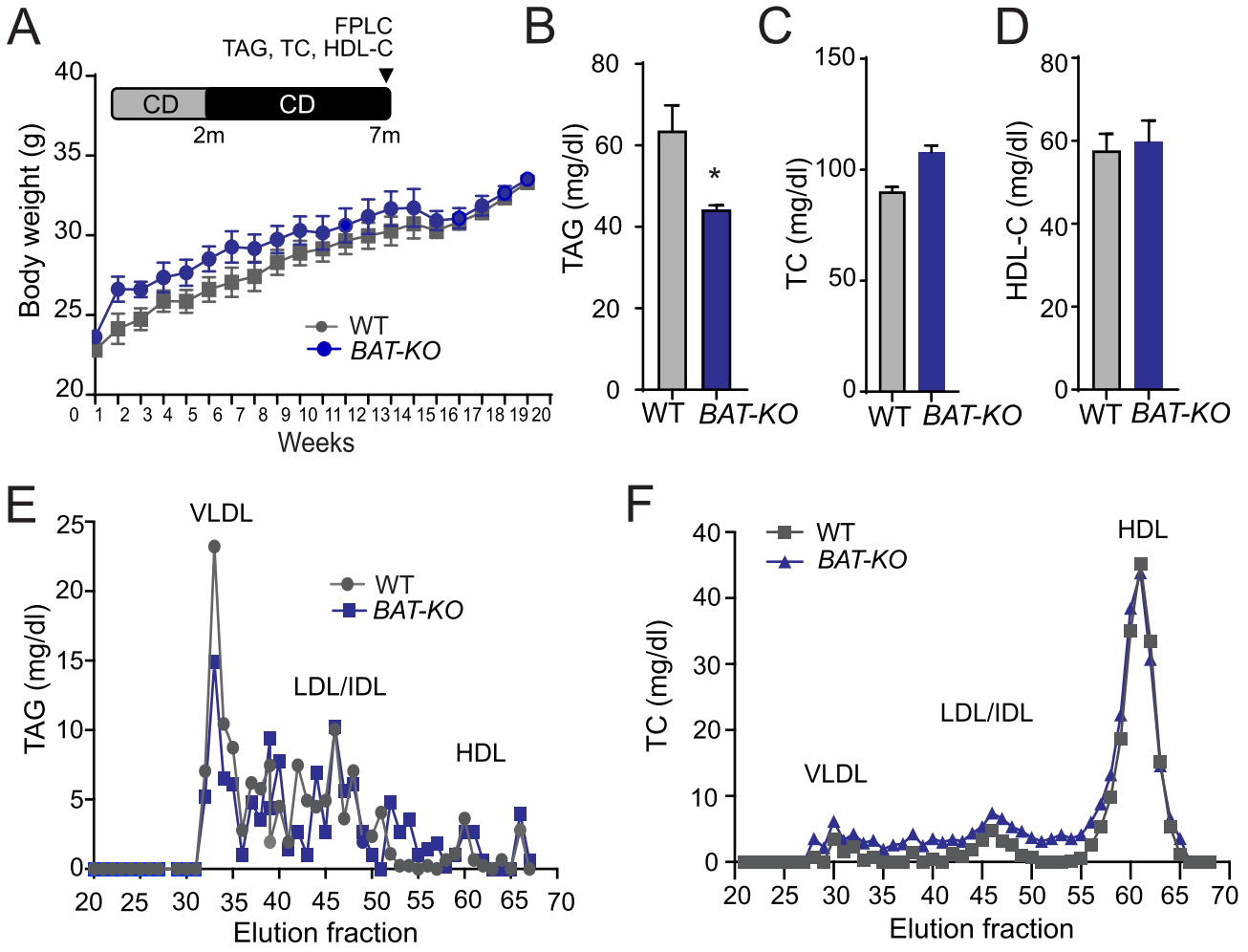

Figure 4: Absence of ANGPTL4 in BAT reduces circulating TAG but does not influence body weight in mice fed a CD. (**A**–**F**) Body weight (**A**), plasma triglyceride (TAG) (**B**), total cholesterol (TC) (**C**), and high-density lipoprotein cholesterol (HDL-C) (**D**) from WT and *BAT-KO* mice fed a chow diet (CD) for 20 weeks (n = 5). (**E** and **F**) TAG (**E**) and TC (**F**) content of FPLC-fractionated lipoproteins from pooled plasma of WT and *BAT-KO* mice fed a CD for 20 weeks (n = 5). All data represent the mean ± S.E.M. and * indicates $P < 0.05$ comparing *BAT-KO* with WT mice using unpaired *t*-test.

3.3. Absence of ANGPTL4 in BAT promotes uptake of TRL derived FA by BAT upon acute cold exposure and enhances cold stimulated thermogenesis

WAT tissue is a specialized lipid storage organ for excess calories, whereas BAT contains large amounts of mitochondria to dissipate chemical energy [36]. Upon cold-stimulation, BAT increases its energy demand and burns lipid to produce heat using UCP1 [12,37,38]. However, the specific role of ANGPTL4 expression in BAT in regulating TRL-derived FA uptake in BAT for energy utilization is still elusive. Thus, we next explored the impact of cold exposure on ANGPTL4 expression in BAT. As expected, acute cold exposure led to a marked reduction in *Angptl4* mRNA (Figure 3A). Based on the significant decrease in *Angptl4* mRNA levels in BAT upon acute cold exposure, we hypothesized that ANGPTL4 might play a role in the catabolism of circulating TAGs in BAT during cold challenge. Indeed, we observed that while the level of circulating TAG was raised with a peak at 2 h and a subsequent decline in WT mice, plasma TAG levels remained persistently low during the postprandial phase in *BAT-KO* mice subjected to cold exposure (Figure 3B). In agreement with these findings, we observed an increased FA delivery to BAT in *BAT-KO* mice compared to WT mice (Figure 3C). Consistent with these changes in lipid metabolism, *BAT-KO* mice maintained their body temperature better during an acute cold stress (Figure 3D). Together, these results suggest that BAT derived ANGPTL4 may play an important role in regulating FA uptake in BAT and thermogenesis upon acute cold exposure.

3.4. Deletion of ANGPTL4 in BAT enhances TAG clearance without altering body weight in mice fed a chow diet

Since we found increased lipid uptake in *BAT-KO* mice, we assumed that it might affect the overall body weight of mice. Thus, we monitored body weight of these mice kept on chow diet (CD) for up to 7 months. We did not find any significant difference in the body weight of *BAT-KO* and WT mice (Figure 4A). As expected by the inhibitory effect of ANGPTL4 on LPL activity, plasma TAGs were markedly reduced in mice lacking ANGPTL4 in BAT (Figure 4B). Circulating levels of TC and HDL-C were comparable in both *BAT-KO* and WT mice (Figure 4C—D). Moreover, FPLC analysis revealed that decreased plasma TAG in *BAT-KO* mice was attributable to VLDL fraction (Figure 4E), whereas cholesterol distribution was similar between the groups (Figure 4F).

3.5. Genetic deletion of ANGPTL4 in BAT dose not influence body weight but improves TAG clearance in mice fed a HFD

While thermogenic activation in BAT leads to beneficial effects on systemic lipid metabolism, these effects are blurred during obesity as a result of metabolic dysfunction of BAT [39]. To understand how BAT derived ANGPTL4 partake in the metabolic response to HFD-induced obesity, we fed WT and *BAT-KO* mice a HFD for 20 weeks to induced obesity and measured metabolic parameters. Interestingly, we did not observe any difference in body weight and fat mass, although circulating TAG was significantly reduced in *BAT-KO* as compared to WT mice (Figure 5A,B). Plasma TC and HDL-C concentrations were similar in both groups of mice (Figure 5C,D). Profiling of lipoprotein

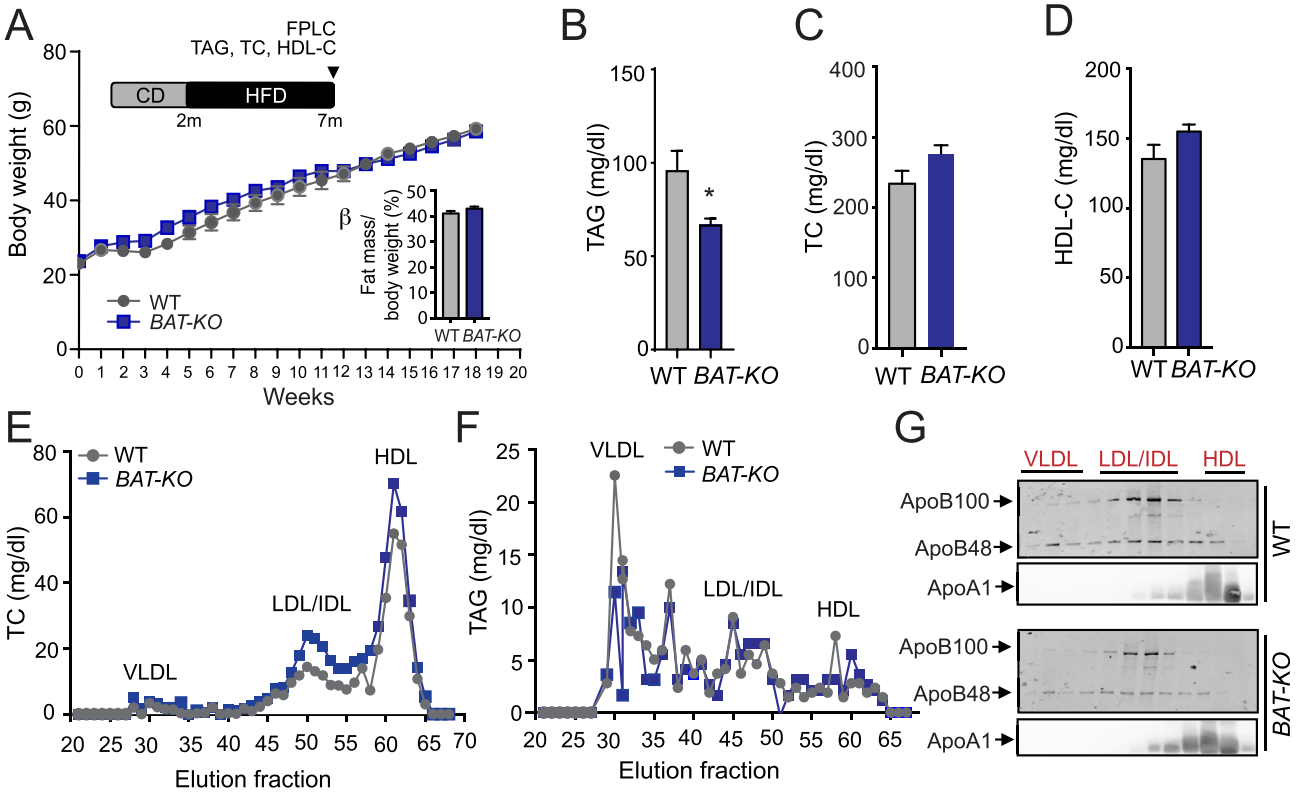

Figure 5: BAT depletion of ANGPTL4 reduces circulating TAG but does not affect body weight in mice fed a HFD. (**A**) Body weight from WT and *BAT-KO* mice fed a high-fat diet (HFD) for 20 weeks. Insert panel shows % fat mass in these mice after 20 weeks on HFD (n = 9). (**B**—**D**) Plasma TAG, (**B**) TC (**C**) and HDL-C (**D**) levels from mice fed a HFD for 20 weeks (n = 5). (**E** and **F**) TC (**E**) and TAG (**F**) content of FPLC-fractionated lipoproteins from pooled plasma of WT and BAT-KO mice fed a HFD for 20 weeks (n = 8). (**G**) Representative western blot analysis of plasma ApoB100, ApoB48, and ApoA1 in the FPLC-fractionated lipoproteins. Lanes 1—12 correspond to the following pooled fractions: 1 (28—30), 2 (31—33), 3 (34—36), 4 (37—39), 5 (40—42), 6 (43—45), 7 (46—48), 8 (49—51), 9 (52—54), 10 (55—57), 11 (58—60), and 12 (61—63). All data represent the mean ± S.E.M. and * indicates $P < 0.05$ comparing *BAT-KO* with WT mice using unpaired *t*-test.

analysis revealed similar distribution of cholesterol amount across different lipoproteins while there was a significant decrease in TAG content in VLDL fraction in mice lacking the expression of ANGPTL4 in BAT (Figure 5E,F). Immunoblotting analysis of ApoB48 and ApoB100 protein content in plasma samples isolated from overnight fasted WT and *BAT-KO* mice exhibited a marked decrease in circulating ApoB lipoproteins (Figure 5G). Additionally, we did not observe any change in the level of ApoA1 protein in HDL fractions in these plasma samples of these mice (Figure 5G), suggesting that absence of ANGPTL4 in BAT accelerates VLDL catabolism and/or clearance but not HDL metabolism.

3.6. Depletion of ANGPTL4 in BAT improves glucose tolerance and insulin sensitivity in short-time HFD fed BAT-KO mice

BAT activation leads to lowered plasma lipid and glucose levels and therefore improves glucose homeostasis in mice [40]. To assess whether the decreased circulating lipids and increased influx of FA in the BAT of *BAT-KO* mice alter glucose metabolism, we performed glucose (GTT) and insulin tolerance tests (ITT) on mice fed a CD. The results showed that absence of ANGPTL4 in BAT does not influence glucose homeostasis (Figure 6A,B). Additionally, it has also been reported that BAT activation normalizes glucose tolerance in HFD-induced obese mice [12]. Therefore, we performed GTT and ITT in mice fed with HFD. Interestingly, we found a markedly improved glucose tolerance in mice fed a HFD for four weeks, suggesting that absence ANGPTL4 in BAT protects against diet-induced glucose intolerance and ameliorates hyperlipidemia (Figure 6C,D). Although lipid-induced insulin resistance usually develops in mice within 4 weeks of HFD feeding, obesity-induced insulin resistance develops after 16 weeks of HFD. Therefore, we next examined whether BAT-KO mice have ameliorated insulin resistance in prolonged administration of HFD (20 weeks) by performing GTT and ITT. We noticed improved glucose clearance during ITT; however, no change was observed in GTT (Figure 6E,F). Together, these observations suggest that the beneficial effects of ANGPTL4 deficiency in BAT in short-term HFD fed mice are attenuated in mice fed a HFD over a long period of time.

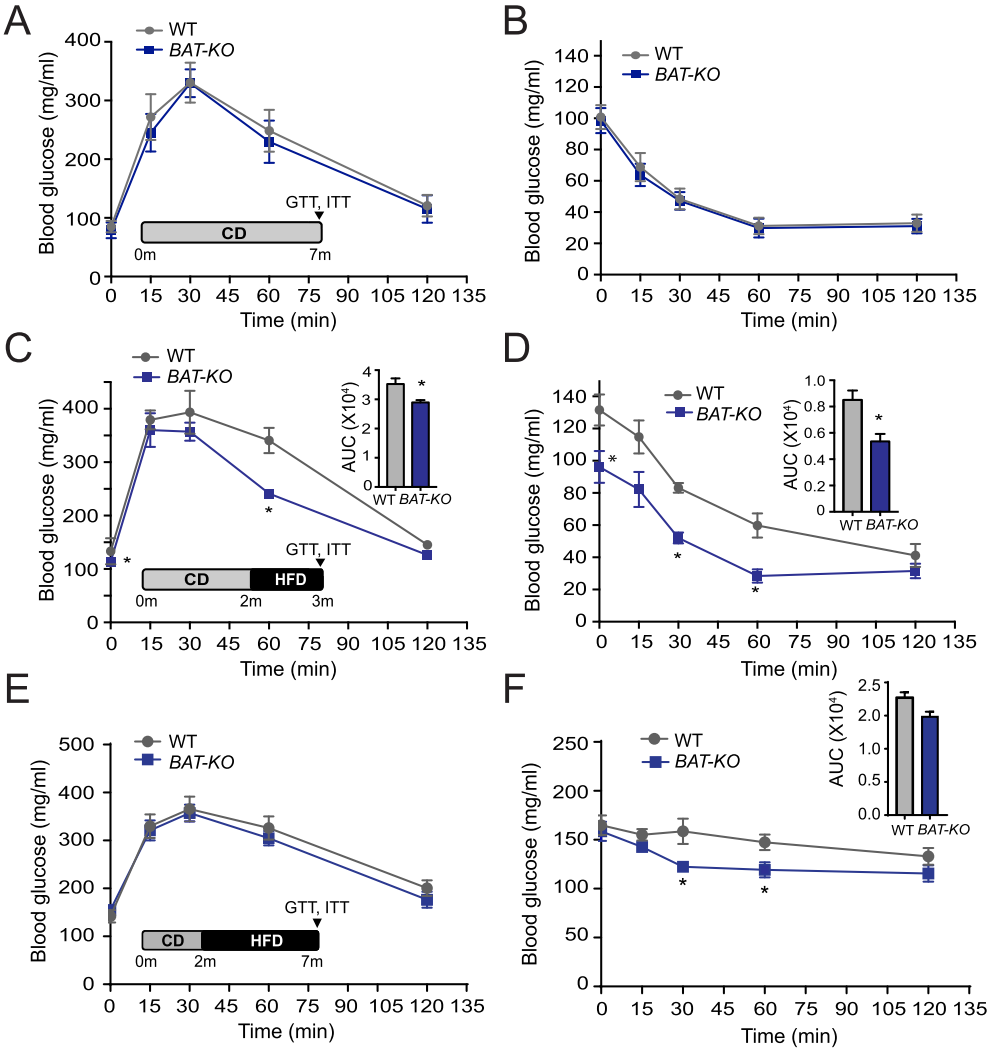

Figure 6: Lack of ANGPTL4 expression in BAT improves glucose and insulin tolerance. (**A**–**F**) Glucose tolerance test (GTT) and insulin tolerance test (ITT) in WT and *BAT-KO* mice fed a CD (n = 5) (**A** and **B**), or a HFD for 4 weeks (n = 5) (**C** and **D**), or a HFD for 20 weeks (n = 5) (**E** and **F**). Inset represents the area under the curve (AUC). All data represent the mean ± S.E.M and * indicates P < 0.05 comparing *BAT-KO* mice with WT mice using unpaired *t*-test.

3.7. Deletion of ANGPTL4 in BAT leads to increased FA oxidation coupled with reduced *de novo* lipogenesis

In spite of an increased influx of FA into BAT, there was no difference in the fat mass composition and the size of brown adipocytes of *BAT-KO* mice as compared to WT mice (Figure 7A). Hence, we speculated that this might occur owing to either accelerated energy utilization through FA oxidation or decreased *de novo* lipogenesis (*DNL*) or a combination of both processes. Interestingly, we observed increased *ex-vivo* FA oxidation in BAT isolated from BAT-KO mice as compared to BAT obtained from WT mice (Figure 7B). Mechanistically, we found that absence of ANGPTL4 in BAT enhanced the expression of thermogenic proteins such as PGC-1α and UCP1 which are responsible for FA oxidation in BAT (Figure 7C). Conversely, DNL was attenuated in *BAT-KO* mice as compared to WT mice (Figure 7D). In agreement with this observation, *Fasn* mRNA levels were significantly reduced in *BAT-KO* mice as compared to WT mice (Figure 7E). These results suggest that absence of ANGLTL4 in BAT influences fat mass by regulating TRL clearance, FA oxidation and DNL.

4. DISCUSSION

BAT can considerably escalate metabolic rate and dissipate large amounts of lipids in a rather short time once stimulated [12,41]. Despite being recently recognized as an important player in regulating lipoprotein metabolism, the mechanism by which BAT catabolizes and enhances the clearance of TRL has not been fully elucidated. In this study, we demonstrated that FA uptake in brown adipocytes is regulated by ANGPTL4 under physiological conditions and during cold-induced thermogenesis. Importantly, absence of ANGPTL4 in brown adipocytes resulted in accelerated TRL catabolism and reduced circulating TAG. Multiple studies have conclusively shown that ANGPTL4 inhibits LPL activity and regulates TAG catabolism [18–20,26,27]. Consistent with these data, we also observed increased plasma TAG clearance in BAT-KO mice challenged with oral lipid. This observation was associated with increased BAT lipid uptake and LPL activity, confirming that BAT specific ANGPTL4 modulates plasma TAG levels. *BAT-KO* mice maintained better body

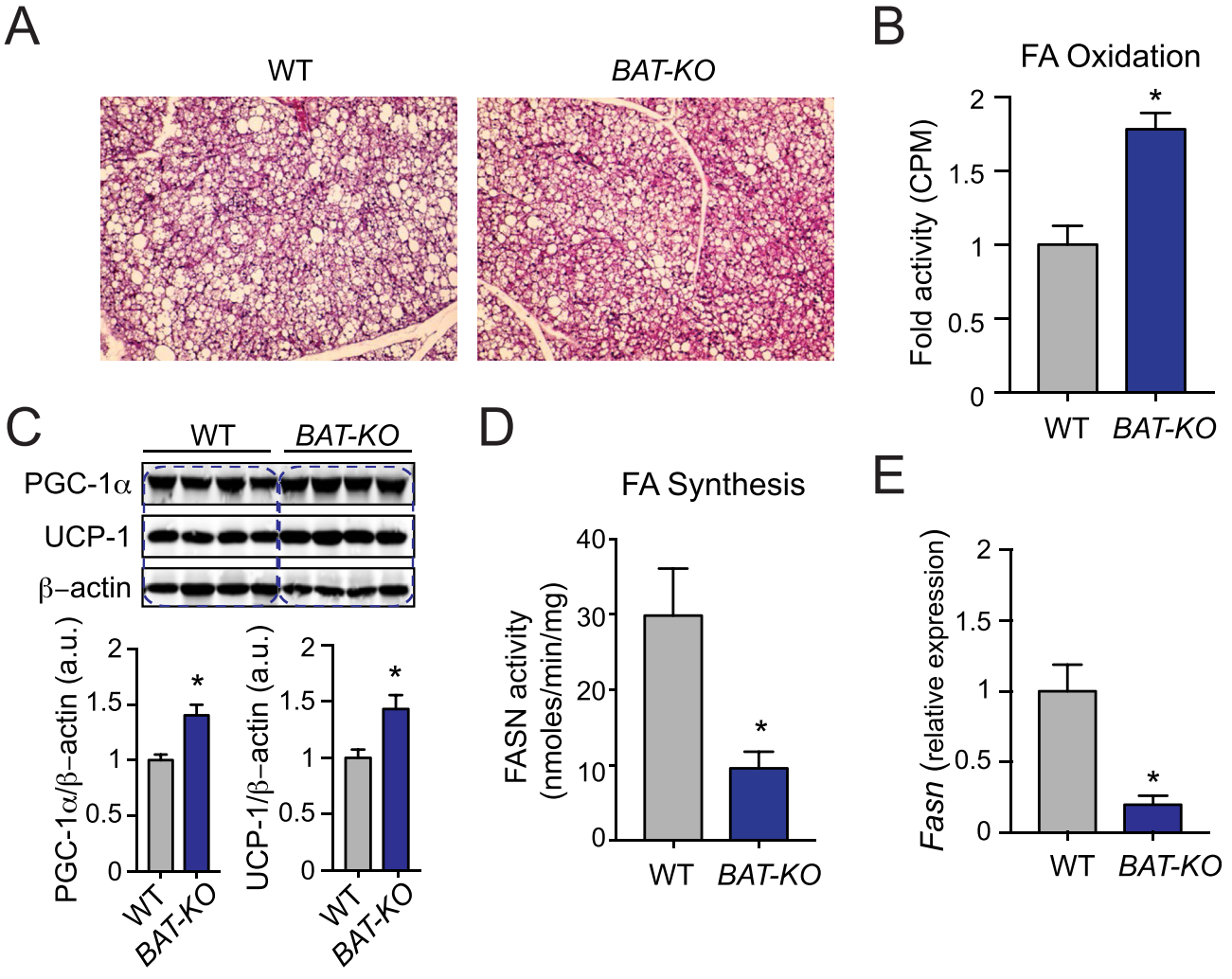

Figure 7: Loss of ANGPTL4 in BAT enhances the expression of genes associated to oxidative metabolism coupled with reduced endogenous lipogenesis. (**A**) Representative H&E stained sections of BAT isolated from WT and *BAT-KO* mice fed a HFD for 20 weeks. (**B**) FA oxidation in isolated BAT from WT and *BAT-KO* mice (n = 6). (**C**) Representative western blot analysis of indicated proteins in BAT from WT and BAT-KO mice fed a HFD for 20 weeks (n = 4) and densitometry analysis of the respective blots. (**D**) Measurement of FASN activity in isolated BAT of WT and *BAT-KO* mice (n = 6). (**E**) qRT-PCR analysis of *Fasn* expression in BAT isolated from WT and *BAT-KO* mice fed a HFD for 20 weeks (n = 3). All data represent the mean ± SEM and * indicates P < 0.05 comparing *BAT-KO* with WT mice using unpaired *t*-test.

temperatures upon cold exposure, indicating that Inhibition of ANGPTL4 in BAT reprogrammed BAT to increase FA uptake from blood for combustion, and eventually stimulated thermogenesis. Recently, it has been reported that ANGPTL4 transgenic mice are cold sensitive and show decreased FA uptake in BAT under cold condition; in contrast, no such change was observed in whole-body knockout mice [42]. It is quite likely that other tissues might also be involved in FA uptake under cold environment in global knockout mice owing to increased LPL activity. Nonetheless, we provided direct evidence that BAT derived ANGPTL4 is indispensable for TRL derived FA uptake in BAT both under cold as well as RT conditions.

Despite an increased uptake of FA by BAT in BAT-KO mice, their fat mass and brown adipocyte size were not increased compared to WT mice. Interestingly, mice lacking the expression of ANGPTL4 in BAT express higher levels of PGC-1α and UCP1 and exhibit higher thermogenic activity owing to the increased FA oxidation. These observations suggest that in the absence of ANGPTL4 in brown adipocytes, TRL catabolism is accelerated and eventually leads to increased uptake of FA in BAT which is simultaneously oxidized to produce energy in form of heat. It is well known that FA acids directly activate UCP1 [43]. Alternatively, the decreased endogenous lipid synthesis (based on FASN activity) in *BAT-KO* brown adipocytes may be an adaptive mechanism to match a greater rate of lipid utilization from circulating triglycerides. Thus, concomitant increase in lipid utilization for oxidation and decrease *de novo* lipogenesis (DNL) may explain the BAT phenotype in the *BAT-KO* mice.

Though glucose and FA are the source of energy for BAT thermogenesis under fasting conditions, FA released from hydrolysis of TAGs appear to be the predominant energy substrate. Previous studies have demonstrated that stimulation of BAT increases glucose uptake in obese, diabetic and lean mice [44]. It has also been reported that in the absence of UCP1, rodents have diabetic phenotype [45]. Consistent with these reports we also found that ANGPTL4 deficiency in BAT improved glucose and insulin tolerance by altering BAT activity (based on increased UCP1 expression). To the best of our knowledge, this is the first study showing that ANGPTL4 derived from BAT regulates glucose homeostasis. The outcomes of previous studies on the effects of ANGPTL4 on glucose metabolism are contradictory. While adenovirus mediated overexpression of ANGPTL4 reduced plasma glucose level and improved glucose tolerance in one study, transgenic overexpression of ANGPTL4 in another study resulted in peripheral insulin resistance which impaired glucose homeostasis [22,46]. Additionally, mice with global depletion of ANGPTL4 displayed improved glucose tolerance during dexamethasone induced hepatic insulin resistance condition [47]. These discrepancies could have resulted from the use of mice with different genetic backgrounds with distinct diabetic phenotypes and varying levels of overexpression of ANGPTL4 in different sites. In addition, ANGPTL4 is expressed by several tissues and global modulation of ANGPTL4 results in extreme metabolic abnormalities upon HFD feeding [48]. Our study uses a unique mouse model targeting metabolically active BAT where ANGPTL4 is highly expressed, and thus might represent a better model for studying glucose homeostasis and targeted therapy.

Taken together, we provide evidence that ANGPTL4 derived from brown adipocytes plays an important role in regulating systemic glucose and lipid metabolism. Furthermore, we discovered a novel function of ANGPTL4 in oxidative metabolism and BAT activation through PGC-1α-UCP1 pathway activation. In particular, mice lacking ANGPTL4 display BAT activation in response to cold stimulation and in HFD-induced obesity, as determined by FA oxidation and UCP1-mediated uncoupling. The detailed mechanism underlying how ANGPTL4 regulates PGC-1α UCP1 activation warrants further investigation.

5. CONCLUSION

Our study dissects the specific contribution of ANGPTL4 in BAT in regulating lipid and glucose metabolism. Using a novel tissue specific knockout mouse model, we demonstrate that ANGPTL4 expression in BAT controls TRL catabolism and circulating TAGs, facilitates FA uptake and improves cold tolerance. Finally, we also provide novel evidences suggesting that ANGPTL4 in BAT promotes FA oxidation and attenuates FA synthesis.

AUTHOR CONTRIBUTIONS

AKS, BA, YS, and CF-H conceived and designed the study and wrote the manuscript. BA, AKS, BC, NR, and LV performed experiments and analyzed data. TLH assisted with experimental design and data interpretation.

ACKNOWLEDGMENTS

This work was supported by grants from the National Institutes of Health (R35HL135820 to CF-H and R01HL105945 and R01HL135012 to YS), the American Heart Association (16EIA27550005 to CF-H; 16GRNT26420047 to YS and 17SDG33110002 to NR), and the Foundation Leducq Transatlantic Network of Excellence in Cardiovascular Research MIRVAD (to CF-H).

CONFLICT OF INTEREST

The authors declare no competing financial interests.

REFERENCES

[1] Ouchi, N., Parker, J.L., Lugus, J.J., Walsh, K., 2011. Adipokines in inflammation and metabolic disease. Nature Reviews Immunology 11:85–97.
[2] Waki, H., Tontonoz, P., 2007. Endocrine functions of adipose tissue. Annual Review of Pathology Mechanisms of Disease 2:31–56.
[3] Friedman, J., 2016. The long road to leptin. Journal of Clinical Investigation 126:4727–4734.
[4] Kusminski, C.M., Bickel, P.E., Scherer, P.E., 2016. Targeting adipose tissue in the treatment of obesity-associated diabetes. Nature Reviews Drug Discovery 15:639–660.
[5] Bremer, A.A., Jialal, I., 2013. Adipose tissue dysfunction in nascent metabolic syndrome. Journal of Obestics 2013:393192.
[6] Bluher, M., 2009. Adipose tissue dysfunction in obesity. Experimental and Clinical Endocrinology & Diabetes 117:241–250.
[7] Cannon, B., Nedergaard, J., 2017. What ignites UCP1? Cell Metabolism 26: 697–698.
[8] Stern, J.H., Scherer, P.E., 2015. Adipose tissue biology in 2014: advances in our understanding of adipose tissue homeostasis. Nature Reviews Endocrinology 11:71–72.
[9] Villarroya, F., Cereijo, R., Villarroya, J., Giralt, M., 2017. Brown adipose tissue as a secretory organ. Nature Reviews Endocrinology 13:26–35.
[10] Cannon, B., Nedergaard, J., 2004. Brown adipose tissue: function and physiological significance. Physiological Reviews 84:277–359.
[11] Rothwell, N.J., Stock, M.J., 1979. A role for brown adipose tissue in diet-induced thermogenesis. Nature 281:31–35.
[12] Bartelt, A., Bruns, O.T., Reimer, R., Hohenberg, H., Ittrich, H., Peldschus, K., et al., 2011. Brown adipose tissue activity controls triglyceride clearance. Nature Medicine 17:200–205.

[13] Fedorenko, A., Lishko, P.V., Kirichok, Y., 2012. Mechanism of fatty-acid-dependent UCP1 uncoupling in brown fat mitochondria. Cell 151:400–413.
[14] Goldberg, I.J., Eckel, R.H., Abumrad, N.A., 2009. Regulation of fatty acid uptake into tissues: lipoprotein lipase- and CD36-mediated pathways. The Journal of Lipid Research 50(Suppl. S86–S90).
[15] Merkel, M., Eckel, R.H., Goldberg, I.J., 2002. Lipoprotein lipase: genetics, lipid uptake, and regulation. The Journal of Lipid Research 43:1997–2006.
[16] Kersten, S., 2014. Physiological regulation of lipoprotein lipase. Biochimica et Biophysica Acta 1841:919–933.
[17] Unal, R., Pokrovskaya, I., Tripathi, P., Monia, B.P., Kern, P.A., Ranganathan, G., 2008. Translational regulation of lipoprotein lipase in adipocytes: depletion of cellular protein kinase Calpha activates binding of the C subunit of protein kinase A to the 3'-untranslated region of the lipoprotein lipase mRNA. Biochemical Journal 413:315–322.
[18] Kersten, S., Mandard, S., Tan, N.S., Escher, P., Metzger, D., Chambon, P., et al., 2000. Characterization of the fasting-induced adipose factor FIAF, a novel peroxisome proliferator-activated receptor target gene. Journal of Biological Chemistry 275:28488–28493.
[19] Zhu, P., Goh, Y.Y., Chin, H.F., Kersten, S., Tan, N.S., 2012. Angiopoietin-like 4: a decade of research. Bioscience Reports 32:211–219.
[20] Sukonina, V., Lookene, A., Olivecrona, T., Olivecrona, G., 2006. Angiopoietin-like protein 4 converts lipoprotein lipase to inactive monomers and modulates lipase activity in adipose tissue. Proceedings of the National Academy of Sciences of the U S A 103:17450–17455.
[21] Zhang, R., 2016. The ANGPTL3-4-8 model, a molecular mechanism for triglyceride trafficking. Open Biology 6:150272.
[22] Mandard, S., Zandbergen, F., van Straten, E., Wahli, W., Kuipers, F., Muller, M., et al., 2006. The fasting-induced adipose factor/angiopoietin-like protein 4 is physically associated with lipoproteins and governs plasma lipid levels and adiposity. Journal of Biological Chemistry 281:934–944.
[23] Georgiadi, A., Wang, Y., Stienstra, R., Tjeerdema, N., Janssen, A., Stalenhoef, A., et al., 2013. Overexpression of angiopoietin-like protein 4 protects against atherosclerosis development. Arteriosclerosis Thrombosis and Vascular Biology 33:1529–1537.
[24] Aryal, B., Rotllan, N., Araldi, E., Ramirez, C.M., He, S., Chousterman, B.G., et al., 2016. ANGPTL4 deficiency in haematopoietic cells promotes monocyte expansion and atherosclerosis progression. Nature Communications 7:12313.
[25] Dijk, W., Kersten, S., 2014. Regulation of lipoprotein lipase by Angptl4. Trends in Endocrinology and Metabolism 25:146–155.
[26] Koster, A., Chao, Y.B., Mosior, M., Ford, A., Gonzalez-DeWhitt, P.A., Hale, J.E., et al., 2005. Transgenic angiopoietin-like (angptl)4 overexpression and targeted disruption of angptl4 and angptl3: regulation of triglyceride metabolism. Endocrinology 146:4943–4950.
[27] Desai, U., Lee, E.C., Chung, K., Gao, C., Gay, J., Key, B., et al., 2007. Lipid-lowering effects of anti-angiopoietin-like 4 antibody recapitulate the lipid phenotype found in angiopoietin-like 4 knockout mice. Proceedings of the National Academy of Sciences of the U S A 104:11766–11771.
[28] Gordts, P.L., Nock, R., Son, N.H., Ramms, B., Lew, I., Gonzales, J.C., et al., 2016. ApoC-III inhibits clearance of triglyceride-rich lipoproteins through LDL family receptors. Journal of Clinical Investigation 126:2855–2866.
[29] Kotas, M.E., Jurczak, M.J., Annicelli, C., Gillum, M.P., Cline, G.W., Shulman, G.I., et al., 2013. Role of caspase-1 in regulation of triglyceride metabolism. Proceedings of the National Academy of Sciences of the U S A 110:4810–4815.
[30] Camporez, J.P., Kanda, S., Petersen, M.C., Jornayvaz, F.R., Samuel, V.T., Bhanot, S., et al., 2015. ApoA5 knockdown improves whole-body insulin sensitivity in high-fat-fed mice by reducing ectopic lipid content. The Journal of Lipid Research 56:526–536.
[31] Iqbal, J., Parks, J.S., Hussain, M.M., 2013. Lipid absorption defects in intestine-specific microsomal triglyceride transfer protein and ATP-binding cassette transporter A1-deficient mice. Journal of Biological Chemistry 288:30432–30444.
[32] Huynh, F.K., Green, M.F., Koves, T.R., Hirschey, M.D., 2014. Measurement of fatty acid oxidation rates in animal tissues and cell lines. Methods Enzymology 542:391–405.
[33] Bays, N.W., Hill, A.D., Kariv, I., 2009. A simplified scintillation proximity assay for fatty acid synthase activity: development and comparison with other FAS activity assays. Journal of Biomolecular Screening 14:636–642.
[34] Haller, J.F., Mintah, I.J., Shihanian, L.M., Stevis, P., Buckler, D., Alexa-Braun, C.A., et al., 2017. ANGPTL8 requires ANGPTL3 to inhibit lipoprotein lipase and plasma triglyceride clearance. The Journal of Lipid Research 58:1166–1173.
[35] Nakajima, K., Nakano, T., Tokita, Y., Nagamine, T., Inazu, A., Kobayashi, J., et al., 2011. Postprandial lipoprotein metabolism: VLDL vs chylomicrons. Clinica Chimica Acta 412:1306–1318.
[36] Cedikova, M., Kripnerova, M., Dvorakova, J., Pitule, P., Grundmanova, M., Babuska, V., et al., 2016. Mitochondria in white, brown, and beige adipocytes. Stem Cells International 2016, 6067349.
[37] Festuccia, W.T., Blanchard, P.G., Deshaies, Y., 2011. Control of brown adipose tissue glucose and lipid metabolism by PPARgamma. Frontiers in Endocrinology 2:84.
[38] McKee, G., Andrews, J.F., 1990. Brown adipose tissue lipid is the main source of energy during arousal of the golden hamster (Mesocricetus auratus). Comparative Biochemistry and Physiology A Comparative Physiology 96:485–488.
[39] Cannon, B., Nedergaard, J., 2010. Metabolic consequences of the presence or absence of the thermogenic capacity of brown adipose tissue in mice (and probably in humans). International Journal of Obesity (London) 34(Suppl. 1):S7–S16.
[40] Thoonen, R., Hindle, A.G., Scherrer-Crosbie, M., 2016. Brown adipose tissue: the heat is on the heart. American Journal of Physiology Heart and Circulatory Physiology 310:H1592–H1605.
[41] Blondin, D.P., Tingelstad, H.C., Noll, C., Frisch, F., Phoenix, S., Guerin, B., et al., 2017. Dietary fatty acid metabolism of brown adipose tissue in cold-acclimated men. Nature Communications 8:14146.
[42] Dijk, W., Heine, M., Vergnes, L., Boon, M.R., Schaart, G., Hesselink, M.K., et al., 2015. ANGPTL4 mediates shuttling of lipid fuel to brown adipose tissue during sustained cold exposure. Elife 4.
[43] Townsend, K.L., Tseng, Y.H., 2014. Brown fat fuel utilization and thermogenesis. Trends in Endocrinology and Metabolism 25:168–177.
[44] Stanford, K.I., Middelbeek, R.J., Townsend, K.L., An, D., Nygaard, E.B., Hitchcox, K.M., et al., 2013. Brown adipose tissue regulates glucose homeostasis and insulin sensitivity. Journal of Clinical Investigation 123:215–223.
[45] Winn, N.C., Vieira-Potter, V.J., Gastecki, M.L., Welly, R.J., Scroggins, R.J., Zidon, T.M., et al., 2017. Loss of UCP1 exacerbates Western diet-induced glycemic dysregulation independent of changes in body weight in female mice. American Journal of Physiology Regulatory Integrative and Comparative Physiology 312:R74–R84.
[46] Xu, A., Lam, M.C., Chan, K.W., Wang, Y., Zhang, J., Hoo, R.L., et al., 2005. Angiopoietin-like protein 4 decreases blood glucose and improves glucose tolerance but induces hyperlipidemia and hepatic steatosis in mice. Proceedings of the National Academy of Sciences of the U S A 102:6086–6091.
[47] Chen, T.C., Benjamin, D.I., Kuo, T., Lee, R.A., Li, M.L., Mar, D.J., et al., 2017. The glucocorticoid-Angptl4-ceramide axis induces insulin resistance through PP2A and PKCzeta. Science Signaling 10.
[48] Lichtenstein, L., Mattijssen, F., de Wit, N.J., Georgiadi, A., Hooiveld, G.J., van der Meer, R., et al., 2010. Angptl4 protects against severe proinflammatory effects of saturated fat by inhibiting fatty acid uptake into mesenteric lymph node macrophages. Cell Metabolism 12:580–592.

